Effect of tetrahydroquinoline derivatives on the intracellular Ca²⁺ homeostasis in breast cancer cells (MCF-7) and its relationship with apoptosis.

Semer Maksoud[1], Adriana Mayora[2], Laura Colman[3], Felipe Sojo[4,5], Adriana A. Pimentel[6], Vladimir V. Kouznetsov[7], Diego R. Merchán-Arenas[7], Ángel H. Romero[8], Francisco Arvelo[4,5], Juan Bautista De Sanctis[9] and Gustavo Benaim[10,11]

[1]Department of Neurology and Experimental Therapeutics and Molecular Imaging Laboratory, Massachusetts General Hospital, MA 02129, USA.

[2]Instituto de Medicina Experimental. Facultad de Medicina. Universidad Central de Venezuela.

[3]Instituto Pasteur, Montevideo, Uruguay.

[4]Centro de Biociencias, Fundación Instituto de Estudios Avanzados (IDEA). Caracas, Venezuela.

[5]Laboratorio de Cultivo de Tejidos y Biología de Tumores, Instituto de Biología Experimental, Universidad Central de Venezuela (UCV), Caracas, Venezuela.

[6]Facultad de Farmacia, Universidad Central de Venezuela. Caracas, Venezuela.

[7]Laboratorio de Química Orgánica y Biomolecular (CMN), Universidad Industrial de Santander. Parque Tecnológico Guatiguara, Piedecuesta. Colombia.

[8]Cátedra de Química General, Facultad de Farmacia, Universidad Central de Venezuela. Caracas, Venezuela.

[9]Institute of Molecular and Translational Medicine. Palacky Unversity. Olomouc. Czech Republic.

[10]Laboratorio de Señalización Celular y Bioquímica de Parásitos. Instituto de Estudios Avanzados (IDEA). Caracas, Venezuela.

[11]Instituto de Biología Experimental, Universidad Central de Venezuela (UCV). Caracas. Venezuela.

Abstract. Tetrahydroquinoline derivatives are interesting structures exhibiting a wide range of biological activities, including antitumor effects. In this investigation, the effect of the synthesized tetrahydroquinolines JS-56 and JS-92 on apoptosis, intracellular Ca^{2+} concentration ($[Ca^{2+}]_i$), and the sarco(endo)plasmic reticulum Ca^{2+}-ATPase (SERCA) activity was determined on MCF-7 breast cancer cells. Colorimetric assays were used to assess MCF-7 cells viability and SERCA activity. Fura-2 and rhodamine 123 were used to measure the intracellular Ca^{2+} concentration and the mitochondrial electrochemical potential, respec-

Corresponding author: Gustavo Benaim . Laboratorio de Señalización Celular y Bioquímica de Parásitos, Instituto de Estudios Avanzados (IDEA) and Instituto de Biología Experimental, Universidad Central de Venezuela (UCV), Caracas, Venezuela. Tel: +584143060359; E-mail: gbenaim@gmail.com

tively. TUNEL assay was used to analyze DNA fragmentation, while caspase activity and NF-κB-dependent gene expression were assessed by luminescence. *In silico* models were used for molecular docking analysis. These compounds increase intracellular Ca^{2+} concentration; the main contribution is the Ca^{2+} entry from the extracellular *milieu*. Both JS-56 and JS-92 inhibit the activity of SERCA and dissipate the mitochondrial electrochemical potential through processes dependent and independent of the Ca^{2+} uptake by this organelle. Furthermore, JS-56 and JS-92 generate cytotoxicity in MCF-7 cells. The effect of JS-92 is higher than JS-56. Both compounds activate caspases 7 and 9, cause DNA fragmentation, and potentiate the effect of phorbol 12-myristate-13-acetate on NF-κB-dependent gene expression. Molecular docking analysis suggests that both compounds have a high interaction for SERCA, similar to thapsigargin. Both tetrahydroquinoline derivatives induced cell death through a combination of apoptotic events, increase $[Ca^{2+}]_i$, and inhibit SERCA activity by direct interaction.

Efecto de derivados de tetrahidroquinolinas sobre la homeostasis del Ca^{2+} intracelular en células de cáncer de mama (MCF-7) y su relación con la apoptosis.

Resumen. Los derivados de tetrahidroquinolina son estructuras interesantes que exhiben una amplia gama de actividades biológicas, incluyendo efectos antitumorales. Se determinó el efecto de las tetrahidroquinolinas sintetizadas JS-56 y JS-92 sobre la apoptosis, concentración intracelular de Ca^{2+} ($[Ca^{2+}]_i$) y la actividad Ca^{2+}-ATPasa del retículo sarco(endo)plásmico (SERCA) en células de cáncer de mama MCF-7. Se usaron ensayos colorimétricos para evaluar la viabilidad de las células MCF-7 y la actividad SERCA. Se emplearon Fura-2 y rodamina 123 para medir la concentración de Ca^{2+} intracelular y el potencial electroquímico mitocondrial, respectivamente. El ensayo TUNEL se utilizó para analizar la fragmentación del ADN, mientras que la actividad de caspasas y la expresión génica dependiente de NF-κB se evaluaron mediante luminiscencia. Modelos *in silico* permitieron el análisis del acoplamiento molecular. Estos compuestos aumentan la concentración de Ca^{2+} intracelular; la principal contribución es la entrada de Ca^{2+} desde el medio extracelular. Tanto JS-56 como JS-92 inhiben la actividad de SERCA y disipan el potencial electroquímico mitocondrial a través de procesos dependientes e independientes de la captación de Ca^{2+} por este orgánulo. Además, JS-56 y JS-92 generan citotoxicidad en células MCF-7. El efecto de JS-92 es mayor que JS-56. Ambos compuestos activan las caspasas 7 y 9, provocan la fragmentación del ADN y potencian el efecto del 12-miristato-13-acetato de forbol en la expresión génica dependiente de NF-κB. El análisis de acoplamiento molecular sugiere que ambos compuestos tienen una alta interacción con SERCA, similar a la tapsigargina. Ambos derivados de tetrahidroquinolina indujeron la muerte celular a través de una combinación de eventos apoptóticos, aumento de $[Ca^{2+}]_i$ e inhibición de la actividad SERCA por interacción directa.

INTRODUCTION

Breast cancer is the most frequently diagnosed cancer and the leading cause of cancer-related death in women worldwide, with an estimated 2.3 million new cases per year and approximately more than 685,000 deaths by 2020 [1]. Among treatments against this disease is the use of tamoxifen (Nolvadex®) for cancer cells expressing estrogen receptors or trastuzumab (Herceptin®) for HER-2+ mammary tumors [2]. Of particular interest, numerous investigations evaluate the potential of natural or synthetic compounds that stimulate apoptosis in breast cancer cells by disturbing intracellular Ca^{2+} homeostasis [3-9].

Ca^{2+} possesses an essential regulatory role in differentiation, secretion, contraction, transcription, phosphorylation, and apoptosis processes. A piece of large cell machinery composed of different proteins and organelles contributes to the regulation of intracellular Ca^{2+} concentration ($[Ca^{2+}]_i$) [10]. Among them is the sarco(endo)plasmic reticulum Ca^{2+}-ATPase (SERCA), which allows active transport and a considerable accumulation of this cation at the endoplasmic reticulum (ER). Active transport maintains $[Ca^{2+}]$ in the ER. This concentration is approximately three orders of magnitude higher (millimolar range) than cytoplasm $[Ca^{2+}]$ (~100 nanomolar), and similar to the extracellular *milieu* [11]. Apoptosis is directly related to Ca^{2+} transfer from ER to mitochondria. Ca^{2+} depletion in ER can generate a phenomenon called "ER stress" in which the reduction of protein folding capacity, and consequent accumulation of these misfolded proteins, initiates different processes promoting cell death [12,13]. The electrophoretic uniporter (MCU) induces Calcium accumulation in the mitochondria. This $[Ca^{2+}]$ increase generates an important change in electrochemical potential ($\Delta\psi_m$) [14] which may enable membrane permeabilization with consequent release of cytochrome c, caspase-9 activation and cell death [15].

In this investigation, the effect of tetrahydroquinolines JS-56 and JS-92 (Fig. 1) was evaluated on Ca^{2+} homeostasis and apoptosis induction in breast cancer cells MCF-7. The tested compounds were prepared from inexpensive and commercially available isatin, 2-aminobenzonitrile (or 4-bromoaniline) and *trans*-isoeugenol, a major constituent of clove oil using a previously published two-step procedure [16,17]. These tetrahydroquinolines have been shown to exert antitumor activity against various cancer cell lines, including MCF-7, SKBR3, PC3 and Hela cells [16,17]; the aim of the study is to ascertain the mechanism of apoptosis induction by the compounds. Both compounds induced an in-
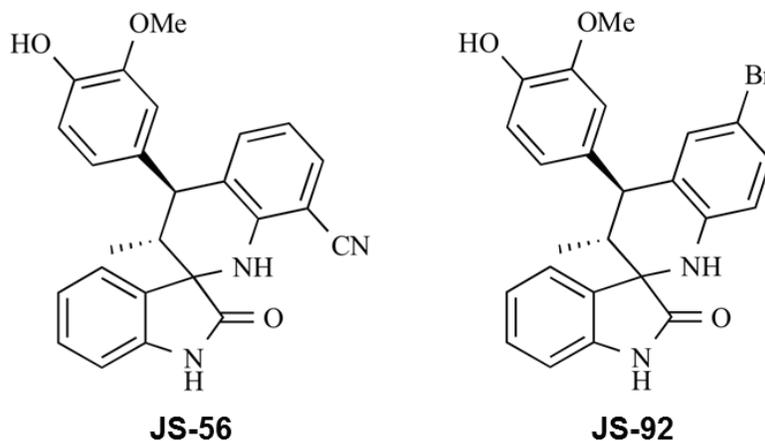

Fig. 1. Chemical structure of the tetrahydroquinolines JS-56 and JS-92.

crease in $[Ca^{2+}]_i$ caused in part through SER-CA inhibition, combined with the dissipation of mitochondrial $\Delta\psi_m$. Molecular docking analysis showed that these compounds have similar ligand-protein interactions with SER-CA when compared to thapsigargin (Tg). Furthermore, these tetrahydroquinolines generated apoptosis via caspase activation and DNA fragmentation. Both compounds enhanced the effect of phorbol 12-myristate-13-acetate (PMA) on the NF-κB-dependent gene expression.

MATERIALS AND METHODS

Chemicals

The preparation of 8'-ciano-4'-(4-hydroxy-3-methoxyphenyl)-3'-methyl-3',4'-dihydro-1'*H*-spiro[indoline-3,2'-quinolin]-2-one (JS-56) and 6'-bromo-4'-(4-hydroxy-3-methoxyphenyl)-3'-methyl-3',4'-dihydro-1'*H*-spiro[indoline-3,2'-quinolin]-2-one (JS-92) was performed by following our previous reports which include the reaction of isatin and 2-aminobenzonitrile or 4-bromoaniline to give the respective ketimine-isatin derivatives and the subsequent acid-catalyzed cycloaddition reaction with *trans*-isoeugenol [16,17]. Both compounds were purified by silica gel column chromatography and obtained as stable solids. Their structures were confirmed by various spectroscopic techniques such as EI-MS, ^{1}H NMR, ^{13}C NMR, and IR, testing each sample as a pure chemical substance in the following biological experiments.

Cell culture

The human breast cancer cell line MCF-7 was grown in Dulbecco's Modified Eagle Medium (DMEM), supplemented with penicillin (100 U/mL), streptomycin (10,000 μg/mL), 1% GlutaMAX™ and 10% fetal bovine serum (FBS). These cells were kept in a humidified incubator at 37°C and in an atmosphere of 5% CO_2.

Cytotoxicity assays

To evaluate the cytotoxicity in MCF-7 cells, the colorimetric reduction assay of 3-(4,5-dimethylthiazol-2-yl)-2,5-diphenyltet-razolium bromide (MTT) was performed [18]. Ten thousand cells were seeded in 96-well plates for 48 h allowing confluence. Cells were exposed to JS-56 and JS-92 for 24 h, at concentrations ranging from 1 to 50 μM. In all cases, both tetrahydroquinolines were dissolved in dimethyl sulfoxide (DMSO). The final concentration of this solvent was equal to or less than 0.5%.

All appropriate controls were developed with 0.5% DMSO. After treatment, cells were incubated with 0.4 mg/mL of MTT for 2 h at 37°C. Then, the supernatant was removed, and the formazan crystals were dissolved by adding 50 μL of DMSO. Absorbance was measured in a multi-detection microplate reader (Sinergy HT, Bio-Tek) at 570 nm. The IC_{50} value was defined as the tetrahydroquinoline concentration causing a 50% reduction in absorbance compared to the control of untreated cells, using the Graphpad Prism 5.0 software.

Measurement of intracellular Ca^{2+} concentration

Measurements of $[Ca^{2+}]_i$ in MCF-7 cells were made using the fluorescent indicator Fura-2, essentially as previously described [19]. Briefly, a suspension of $1x10^6$ cells/mL was prepared in a medium containing 138 mM NaCl, 5 mM KCl, 1 mM $MgCl_2$, 1.5 mM $CaCl_2$, 5 mM glucose, 10 mM HEPES and 0.1% albumin (extracellular medium), loading cells with 200 μM sulfinpyrazone, 0.025% pluronic acid, 0.1% albumin, and 2 μM Fura 2 acetoxymethyl ester (Fura 2-AM) for 30 min at 25°C, in darkness and constant agitation. After loading, cells were incubated for 15 minutes in the extracellular medium and washed again using the same solution. When indicated, these experiments were also performed using the same wash buffer but without $CaCl_2$ (by addition of 2 mM EGTA). Fura-2 fluorescence on loaded cells suspension was monitored through a Perkin Elmer LS 55 spectrofluorimeter with a chopper device. The excitation wavelengths were set at 340 and 380 nm, while the emission was

measured at 510 nm. All experiments were carried out at 30°C, with constant agitation in a stirred cuvette.

Intracellular Ca^{2+} was calculated according to Grynkiewicz et al. [20], using the following equation: $[Ca^{2+}]_I = K_d \times (R-R_{min}/R_{max}-R) \times F_{min(380)}/F_{max(380)}$ where Kd is the dissociation constant of Fura-2 (224 nM). R is the ratio of emission fluorescence intensities to excitation lengths of 340/380 nm. R_{min} and R_{max} are ratios at 0 Ca^{2+} (6 µM digitonin plus 4 mM EGTA) and saturating Ca^{2+} (2 mM $CaCl_2$), respectively. $F_{min(380)}/F_{max(380)}$ are fluorescent values of cells exposed to digitonin plus 4 mM EGTA and 2 mM $CaCl_2$, representing minimal and maximal fluorescent values.

Purification of Ca²⁺-ATPase from the sarcoplasmic reticulum

The sarcoplasmic reticulum was obtained from the white skeletal muscle of the hind legs of rabbits, according to the method described by Eletr and Inesi [21]. The vesicles derived from the sarcoplasmic reticulum are highly enriched in Ca^{2+}-ATPase (approximately 90%). To avoid Ca^{2+} retention in the lumen of the vesicles, the ionophore A-23187 (1 µM) was added.

Evaluation of SERCA activity

The purified enzyme (2 µg/mL) was incubated for 45 min at 37°C and continuous agitation in a final volume of 250 µL of a buffer containing 100 mM KCl, 20 mM MOPS-Tris (pH 7.0), 1 mM EGTA, 10 mM $MgCl_2$, 4 mM ATP, 1 µM A23817 and 1 mM $CaCl_2$, obtaining 10 µM of Ca^{2+} in the medium and reaching an optimal activity of the enzyme. Inorganic phosphate production was quantified using the Fiske and Subbarow [22] colorimetric assay, modified by applying ferrous sulfate as a reducing agent [23].

Determination of the mitochondrial electrochemical potential (Δψm)

Mitochondrial membrane potential changes were measured using the fluorescent marker rhodamine 123, as previously described [24], with the modifications introduced by Pimentel et al. [6]. Rhodamine 123 is a cationic fluorescent dye that allows the evaluation of the electrochemical potential of this organelle when distributed according to the $\Delta\psi_m$. Rhodamine has a maximum excitation peak of 488 nm and a maximum emission peak of 530 nm. For these experiments 3×10^5 cells/mL were resuspended in a medium containing 138 mM NaCl, 5 mM KCl, 1 mM $MgCl_2$, 1.5 mM $CaCl_2$, 5 mM glucose, 10 mM HEPES-KOH, pH 7.4 and then loaded with rhodamine 123 (20 µg/mL) for 45 min at 30°C. All measurements were made on a HITACHI-L-7000 spectrofluorimeter at 30°C with continuous stirring.

Determination of caspases 7 and 9 activity

We used Caspase-Glo 3/7 and Caspase-Glo 9 kits (Promega, Madison, WI) and developed the respective tests following the manufacturer's instructions. Since MCF-7 cells do not possess caspase 3 [25], the results shown correspond to the effect of the different compounds on caspase 7 activity. In a 96-well plate, 10,000 cells/well were seeded and incubated for 48 h at 37°C in a 5% CO_2 atmosphere. Then, cells were exposed to different treatments for 24 h. Then, the cells were lysed, and the luminescence was measured with a multidetector microplate reader (Synergy HT, Bio-Tek). Staurosporine (Stau, 1 µM) was applied as an apoptosis activator (positive control), and 0.5% DMSO was used as a negative control.

Determination of DNA fragmentation

DNA fragmentation was analyzed through the "dead-end fluorimetric TUNEL (TdT-mediated dUTP Nick-End labeling) system" (Promega) kit. Cells were double-labeled with Fluorescein-12-dUTP (a specific marker of fragmented DNA) and propidium iodide (DNA marker). According to manufacturing instructions, changes in fluorescence intensity were detected by flow cytometry (Epics XL Beckman Coulter, FL). Cells incubated with staurosporine (1 µM) were used as a positive control.

Analysis of NF-κB-dependent gene expression

In this assay, HeLa tumor cells transfected with a luciferase reporter gene whose expression is under control of a modified IL-6 promoter, which only contains a critical binding site for NF-κB, were used. The luciferase activity was determined in a luminometer. Five thousand cells/well were seeded in 96-well plates and incubated for 48 h. Subsequently, the cells were exposed to all treatments and corresponding controls for 24 h. Then, the cells were lysed, the luciferase substrate was added, and the product was quantified by luminescence. Incubation with culture medium represents the negative control while phorbol 12-myristate 13-acetate (100 nM) was used as a positive control.

Molecular docking procedure

A 3D crystal structure from SERCA in complex with BHQ (2,5-ditert-butylbenzene-1,4-diol) and Tg was downloaded from Protein Data Bank under PDB code 2AGV. The protein corresponds to sarco(endo)plasmic reticulum Ca^{2+}-ATPase from *Oryctolagus cuniculus* species, and it was crystallized with a resolution of 2.4 Å [26]. The protein presented six co-crystallized chemical ligands: two molecules of BHQ, two molecules of Tg, and two sodium atoms. Four active sites (two for BHQ and the other two for Tg) were generated on the protein: two on α-chain and the other two on β-chain. The 3D structure was imported into the Swiss-PdbViewer v4.0.1 software [27]. Hydrogen atoms were added to the protein structure, and minimization calculations were carried out on protein structure via AMBER force field, using the conjugate gradient method with an RMA gradient of 0.01 kcal/Åmol on Swiss-PdbViewer v4.0.1 software. The prepared protein was exported to an ArgusLab v.4.0.1 program package and saved as an Agl document. Four active sites were constructed on the SERCA protein derived from BHQ and Tg inhibitors. It is well documented that both compounds, BHQ and Tg, act as SERCA inhibitors. Specifically, BHQ is an L-type Ca^{2+} channel inhibitor, blocks Ca^{2+}

transport by inducing superoxide anion production [28]. On the contrary, Tg inhibits all SERCA isozymes at similar concentrations[29]. Both inhibitors are bound to the transmembrane domain of the enzyme close to the membrane/cytosolic interface.

Once the protein was prepared, the two tested tetrahydroquinolines JS56 and JS92 were built using ArgusLab v4.0 [30], optimizing their respective geometries employing B3LYP/6-31G(d,p) [31]. Then, molecular docking of the two compounds and crystallized inhibitors (BHQ and TG) over the four active SERCA sites was performed employing the ArgusLab (v4.0.1) package program under Windows 7.0 environment, applying AMBER force field. The docking was achieved through their respective grid map dimensions and a grid point spacing of 0.375 Å. A flexible ligand model was used in the docking and subsequent optimization scheme. Different orientations of the ligands were scanned and ranked from their energy scores. Reproducibility of the calculated affinity and the minimum energy pose was evaluated through 10 replicates for each quinoline and crystallized inhibitor (BHQ or TS) [32]. The ChemScore scoring function was selected for the evaluation of ligand binding modes. Settings for genetic algorithm runs were kept at their default values; that is, the population size was 100, the selection pressure 1.1, and the number of operations was 100,000. Affinity energy is reported as the mean of the 10 replicates. The lowest energy poses (strongest-docking) for each ligand in each target protein are summarized in Table 1.

RESULTS

Effect of tetrahydroquinolines JS-56 and JS-92 on cytotoxicity in MCF-7 cells

First, the possible cytotoxicity generated by JS-56 and JS-92 on MCF-7 breast cancer cells was evaluated through an MTT assay after being treated for 24 h with different concentrations of these tetrahydroquinolines. It can be observed (Fig. 2) that both compounds

Table 1
Binding energies (kcal/mol), H-interactions, and hydrophobic interactions from molecular docking on the four studied active sites.

| Binding site	Molecule	Binding energy (kcal/mol)	*H*-interactions (Å)	Intermolecular interactions
TG1	JS-56	-13.1366	Two hydrogen bonding (2.8596 and 2.1804 Å) between the phenolic hydrogen of the ligand and Ile-829 residue.	a) H-π interaction with Phe-834 and Phe-256. b) Hydrophobic interactions with Met-838, Tyr-837, Phe-834, Ile-829, Leu-828, Pro-827, Leu-828, Ile-765, Gln-259, Leu-260 and Val-263.
	JS-92	-12.5189	Hydrogen bonding (2.8988 Å) between the phenolic hydrogen of the ligand and Phe-834 residue	a) H-π interaction with Phe-236 and Phe-834. b) Hydrophobic interactions with Met838, Ile829, Pro827, Leu828, and 765Ile.
	Tg	-14.1626	No hydrogen bonding	a) No π-π interactions. b) Hydrophobic interactions with Met-838, Phe-834, Ile-829, Leu-828, Pro-827, Phe-776, Val-773, Val-772, Val-769, Asn-768, Ile-765, Ile-761, Pro-308, Ile-267, Val-263, Leu-260, Gln-259, Phe-256, Leu-253, Leu-249 residues.
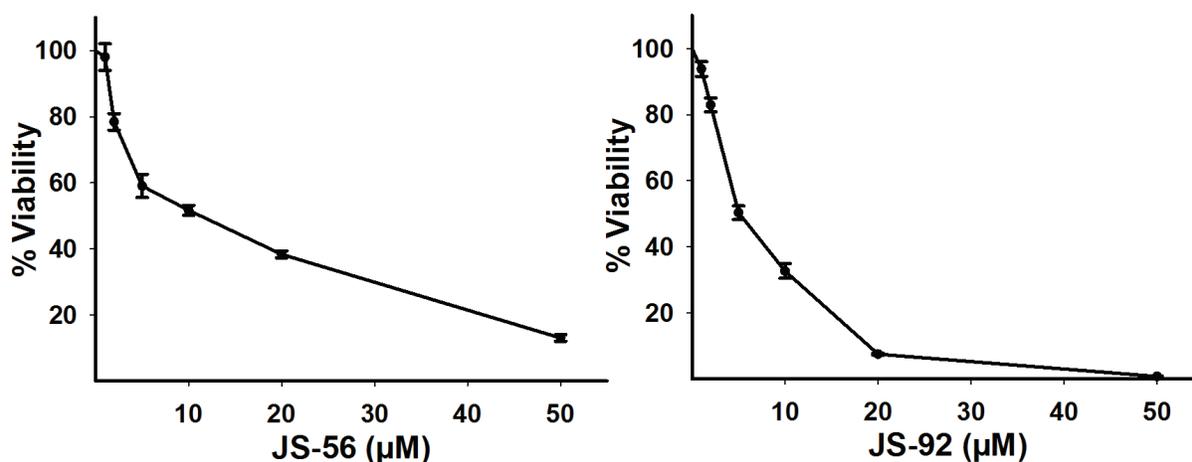
Fig. 2. Effect of tetrahydroquinolines JS-56 and JS-92 on MCF-7 cell viability. MCF-7 cells were treated with different concentrations of these compounds. Each point represents the mean ± SD of three independent experiments. IC50 values obtained for JS-56 and JS-92 were 9.74 μM and 5.03 μM, respectively.

induced cytotoxicity in MCF-7 cells in a dose-dependent manner, with an IC_{50} of 9.74 μM and 5.03 μM for JS-56 and JS-92, respectively. At a concentration of 50 μM, JS-56 decreased cell viability by approximately 88%. At the same time, JS-92 exerted a more substantial effect than JS-56 on this cell line, being able to reduce almost 100% of MCF-7 cell viability at the same concentration.

Effect of tetrahydroquinolines JS-56 and JS-92 on intracellular Ca^{2+} mobilization

To study the effect of these tetrahydroquinolines on the $[Ca^{2+}]_i$, cells were loaded with the Ca^{2+} fluorescent indicator Fura-2. The addition of JS-56 induced a rapid increase in $[Ca^{2+}]_i$, reaching a peak followed by a continuous decrease (Fig. 3A), as a consequence of $[Ca^{2+}]_i$ regulation carried out by the cellular homeostatic machinery until it reached a new steady-state Ca^{2+} level, which is greater than

the original basal level. This response is characteristic of compounds capable of inducing the release of Ca^{2+} from the ER, with the consequent opening of plasma membrane Ca^{2+} channels (SOCE) activated by emptying this intracellular reservoir [19,33]. The effect observed upon the addition of thapsigargin (Tg) (Fig. 3B), a potent SERCA inhibitor, was similar to that observed with JS-56. However, the maximum Ca^{2+} peak achieved with Tg was higher than JS-56. Additionally, when comparing Figures 3A and 3B, the addition of Tg after JS-56 (Fig. 3A) still induced a slight increase in $[Ca^{2+}]_i$. However, the tetrahydroquinoline did not exert any discernible effect after Tg addition (Fig. 3B).

The same experiments were performed in the absence of extracellular Ca^{2+} to determine the origin of the cation increase. Under these experimental conditions, the maximum Ca^{2+} peaks obtained with JS-56 (Fig. 3C) or Tg (Fig. 3D) were considerably lower than
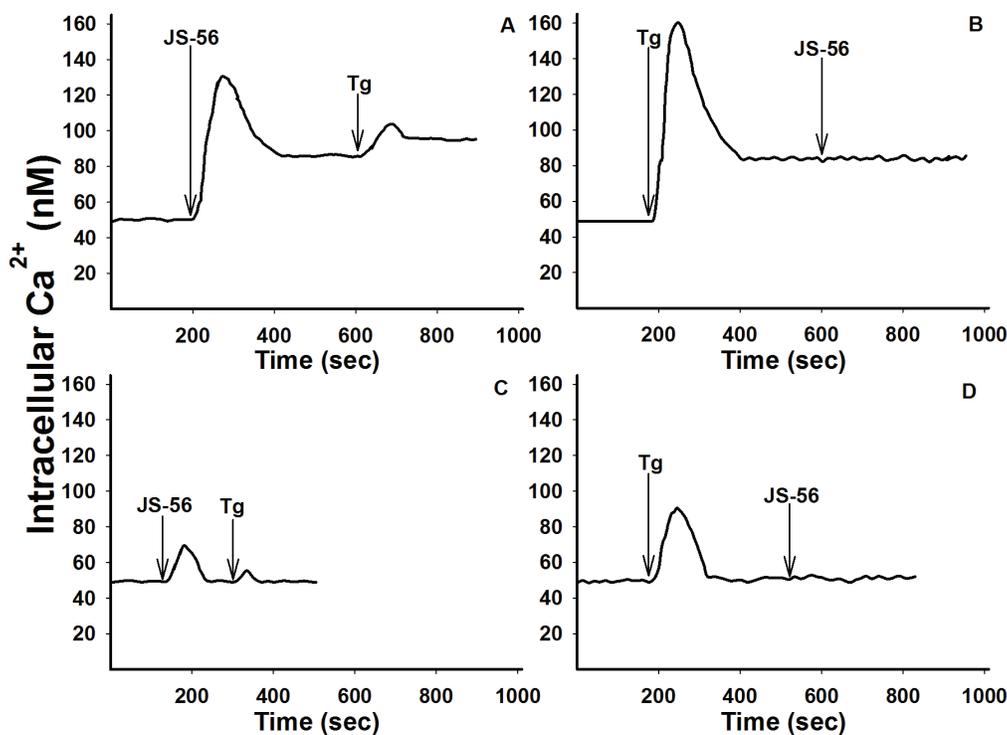
Fig. 3. Effect of tetrahydroquinoline JS-56 and thapsigargin (Tg) on $[Ca^{2+}]i$ in MCF-7 cells. The arrows indicate the moment in which JS-56 (20 μM) and Tg (2 μM) were added, in the presence (Fig. A and B) or absence (EGTA, Fig. C and D) of 2 mM $CaCl_2$. The curves are representative of at least three independent experiments.

those reached in the presence of extracellular Ca^{2+} (Figs. 3A and 3B). Furthermore, the Ca^{2+} levels obtained, after the maximum peak and the subsequent decrease, were equal to the basal levels (Figs. 3C and 3D). Moreover, when Tg was added after JS-56, a minimal rise in $[Ca^{2+}]_i$ was detected, indicating again that, different from Tg, the tetrahydroquinoline was not able to release all the Ca^{2+} from the ER (Fig. 3D). Likewise, the effect of the tetrahydroquinoline JS-92 was evaluated under the same experimental conditions, obtaining essentially the same overall results, as can be observed in Fig. 4.

Effect of tetrahydroquinolines JS-56 and JS-92 on SERCA activity

To identify a possible mechanism of action of these compounds, which could explain their effect on the increase in $[Ca^{2+}]_i$, the ability to inhibit SERCA activity was examined, considering that the results obtained were very similar to those found by the use

of Tg. Fig. 5 shows the effect of increasing concentrations of JS-56 and JS-92 on ATPase activity. Both tetrahydroquinolines inhibited SERCA activity in a dose-dependent manner. The maximum inhibitory effect of JS-56 and JS-92 on SERCA activity was 56 and 51%, respectively. Albeit none of the tetrahydroquinolines could completely inhibit the SERCA activity, these results demonstrate that part of the effect of these compounds on $[Ca^{2+}]_i$ elevation was undoubtedly due to SERCA activity inhibition.

Effect of tetrahydroquinolines JS-56 and JS-92 on the mitochondrial electrochemical potential

Mitochondria use their electrochemical membrane potential ($\Delta\psi_m$) to accumulate Ca^{2+} through the electrophoretic Ca^{2+} uniporter (MCU). The effects of the tetrahydroquinolines and Tg on the mitochondrial $\Delta\psi$ were studied by using the fluorescent marker rhodamine 123. This fluorescent indica-
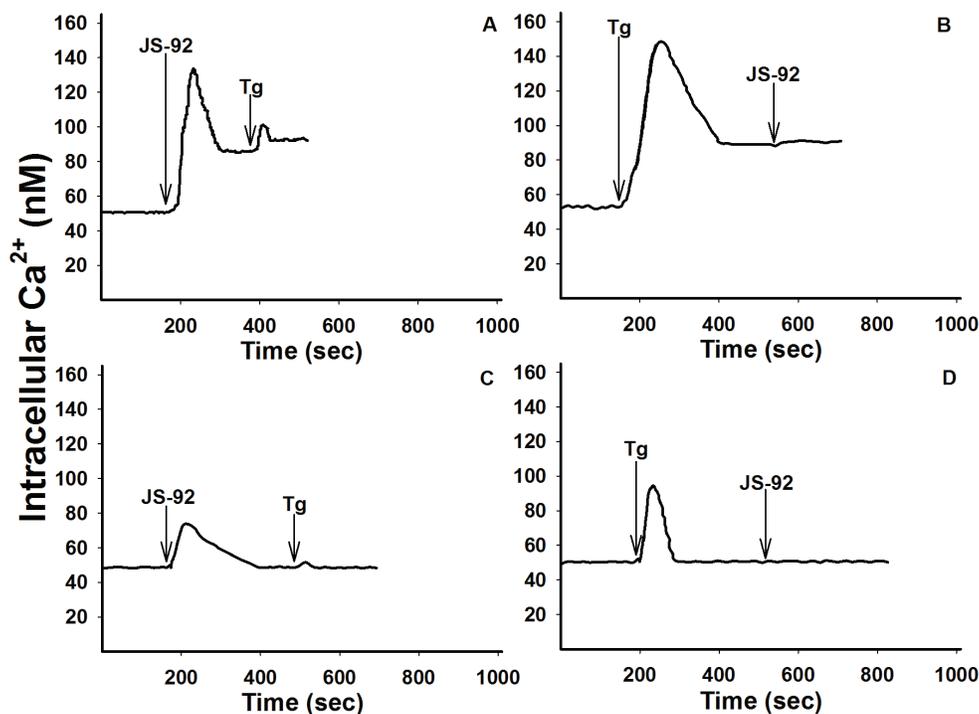

Fig. 4. Effect of tetrahydroquinoline JS-92 and thapsigargin (Tg) on $[Ca^{2+}]i$ in MCF-7 cells. The arrows indicate the addition of JS-92 (20 μM) and Tg (2 μM), in the presence (Fig. A and B) or absence (EGTA, Fig. C and D) of 2 mM $CaCl_2$. The curves are representative of at least three independent experiments.
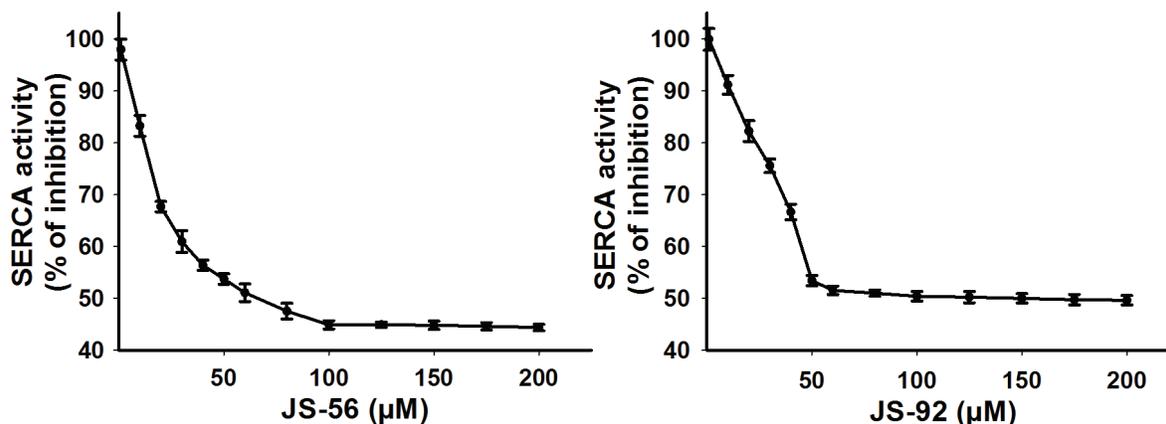
Fig. 5. Effect of tetrahydroquinolines JS-56 and JS-92 on SERCA activity. Each point represents the mean ± SD of three independent experiments.

tor accumulates in the mitochondrial matrix according to the electrochemical gradient. Thus, an increase in fluorescence can be observed due to the mitochondrial H^+ gradient dissipation, concomitantly with the release of rhodamine 123 from the mitochondria to the cytoplasm and then to the extracellular milieu. Results from Fig. 6 demonstrate that both JS-56 and JS-92 (20 μM) and Tg (2 μM) produced a rapid and pronounced elevation in fluorescence due to rhodamine 123 release from mitochondria. However, the increment in rhodamine 123 fluorescence caused by Tg was more significant than those produced by the tetrahydroquinolines (Figs. 6B and 6D). It can also be noticed that JS-92 (Fig. 6C) generated an elevation of rhodamine 123 fluorescence higher than JS-56 (Fig. 6A).

The effect of Tg after the addition of the tetrahydroquinolines was less pronounced (Figs. 6A and 6C). It is worthwhile to mention that this fluorescence elevation with both Tg and tetrahydroquinolines was expected since it was due to the partial dissipation of mitochondrial $\Delta\psi$, generated by the entry of Ca^{2+} released from the ER[6]. On the other hand, after Tg application, the addition of JS-56 and JS-92 led to an additional boost in fluorescence (Figs. 6B and 6D), indicating a superior $\Delta\psi$ dissipation, which cannot be merely explained by the en-

trance of Ca^{2+} released from the ER. Thus, these results suggest that both tetrahydroquinolines can directly affect the mitochondria by Ca^{2+}-independent mechanisms. As expected, the positive control, carbonyl cyanide-4-(trifluoromethoxy)phenylhydrazone (FCCP), generated a complete collapse of the electrochemical gradient.

Effect of tetrahydroquinolines JS-56 and JS-92 on the activity of caspases 7 and 9

We then evaluated the possible effect of these tetrahydroquinolines on the induction of apoptosis in MCF-7 cells. Accordingly, the activation of caspase 9, a known caspase that initiates apoptosis, was assessed. The 1/2 IC_{50}, IC_{50}, and 2 IC_{50} obtained in the MTT assay were used for both compounds. As shown in Fig. 7 (upper panel), both JS-56 and JS-92 significantly enhanced the activity of caspase-9 compared to the control in a dose-dependent manner. Sphingosine (Sph), which promotes an increase in $[Ca^{2+}]_i$ in MCF-7 cells [33], and 2,5-di-t-butyl-1,4-benzohydroquinone (BHQ), a known SERCA reversible-inhibitor [34], also elevated the activity of this initiating caspase. The positive control Stau, which activates apoptosis in MCF-7 cells [35], effectively activated caspase 9 at a level similar to the IC_{50} of the tetrahydroquinolines.
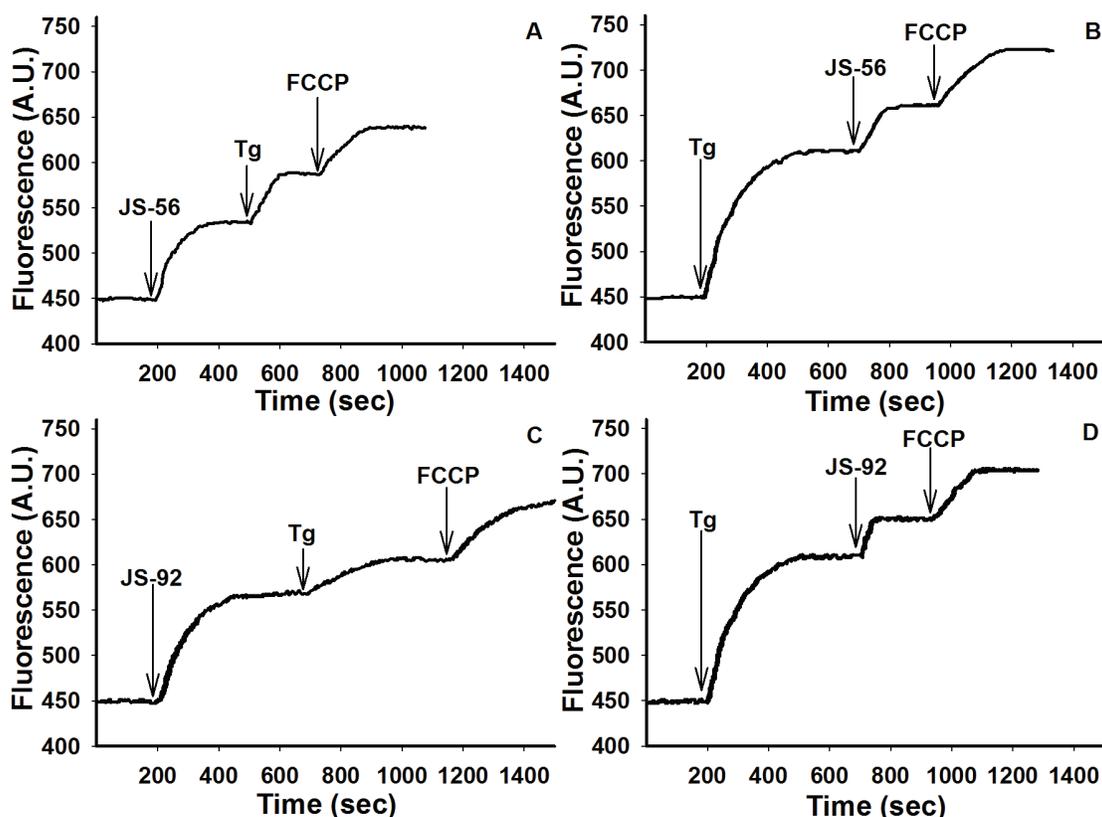
Fig. 6. Effect of tetrahydroquinolines JS-56 and JS-92 on the mitochondrial electrochemical potential in MCF-7 cells. The fluorescent marker rhodamine 123 was used for these experiments, expressing results in arbitrary units (AU) of fluorescence. The arrows indicate the moment of the addition of the different effectors: JS-56 or JS-92 (20 μM), thapsigargin (Tg, 2 μM), and FCCP (10 μM). The curves are representative of at least three independent experiments.

Likewise, treatment of MCF-7 cells with both tetrahydroquinolines raised the activity of caspase 7 (Fig. 7, lower panel). Similar results were detected with the positive control Stau and the SERCA inhibitor BHQ. The activation-induced by JS-92 was slightly higher compared to the rest of the compounds. This effector caspase will be responsible for cleaving specific cell targets to promote apoptosis in these cells.

Effect of tetrahydroquinolines JS-56 and JS-92 on DNA fragmentation

An apoptotic cell is typically characterized by: changes in cell morphology, phosphatidylserine externalization, cytoplasm contraction, shrinkage of the nucleus, and DNA fragmentation [15]. As a complement to the results obtained in caspases 7 and 9 activity assays, DNA fragmentation was analyzed through a TUNEL assay using Stau as a positive control. In Fig. 8, cells were divided into four populations displaying the percentage of cells in necrosis (propidium iodide, IP+), apoptosis (fluorescein isothiocyanate, FITC+), and alive (negative for both markers); apoptotic cells can either be IP- or IP+. Apoptotic cells exhibit DNA fragmentation, which allows FITC incorporation. However, a subset of these apoptotic cells is also IP+, denoting that these also have a loss of plasma membrane integrity, corresponding to a

later stage of apoptosis in which cells can no longer control the passage of elements across the membrane, with eventual cell lysis in the final stage. The quantitative data is represented in Table 2.
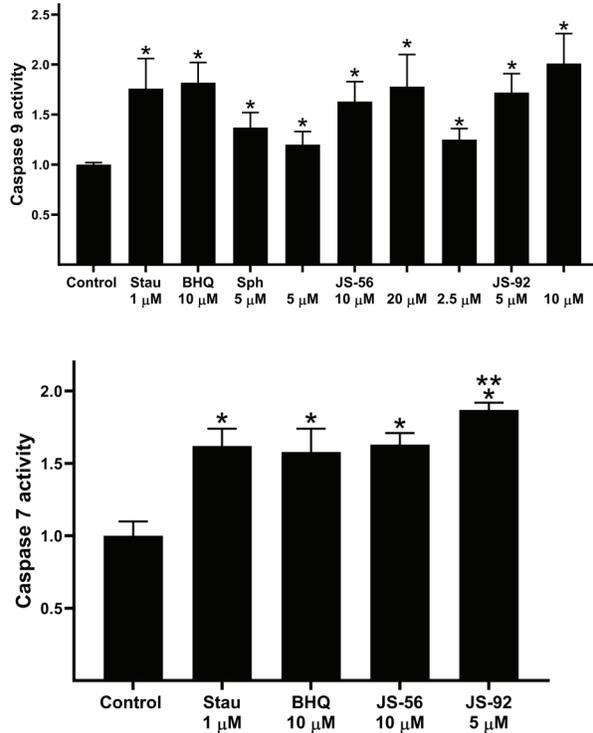
Fig. 7. Effect of tetrahydroquinolines JS-56 and JS-92 on the activity of caspases 9 (initiator) and 7 (effector). Stau (staurosporine), BHQ (2,5-di-t-butyl-1,4-benzohydroquinone) and Sph (sphingosine). The bars represent the mean ± SD derived from three independent experiments. * and ** $p < 0.05$ compared to the control of untreated cells or treated with JS-56, respectively.

JS-56 treatment (10 μM) for 24 h induced apoptosis, with 65.9% of FITC⁺ IP⁻ cells in this stage and only 4.3% of FITC⁺ IP⁺ cells. Treatment with Stau (1 μM) and JS-92 (5 μM) produced a significant percentage of FITC⁺ IP⁻ (31.5 and 46.5% for Stau and JS-92, respectively) and FITC⁺ IP⁺ cells (60.6 and 35.5% for Stau and JS-92, respectively). Hence, JS-92 has a more potent effect than JS-56, which measurements of caspase activity have also evidenced. These results are statistically significant compared to the negative control (DMSO-treated MCF-7 cells).

Effect of tetrahydroquinolines JS-56 and JS-92 on NF-κB-dependent gene expression

The nuclear transcription factor NF-κB regulates numerous genes involved in multiple cellular processes such as apoptosis, cell proliferation, and differentiation. To evaluate NF-κB-dependent gene expression, HeLa tumor cells transfected with a luciferase reporter gene under the control of IL-6 promoter, which contains critical binding sites for NF-κB, were used.

Tetrahydroquinolines JS-56 and JS-92, when added alone, were not able to increase the NF-κB-dependent gene expression, with values similar to those observed in the negative control (Fig. 9). The luminescence measured in the negative control corresponds to the basal NF-κB-dependent gene expression on MCF-7 cells. The NF-κB-dependent gene expression is elevated when cells were treated with 100 nM of PMA; it has been

Table 2
Percentage of living, apoptotic, and necrotic cells after treatment with JS-56 and JS-92.

Treatment group	Percentage			
	Living cells	Apoptosis (IP-)	Apoptosis (IP+)	Necrosis
Control DMSO	93.5 ± 4.6	0.9 ± 0.6	0.1 ± 0.1	4.1 ± 1.2
Staurosporine	3.9 ± 1.3	31.5 ± 7.5	60.6 ± 6.8	1.2 ± 0.5
JS-56	25.5 ± 9.3	65.9 ± 4.7	4.3 ± 2.8	1.9 ± 1.6
JS-92	14.6 ± 6.3	46.5 ± 5.5	35.5 ± 4.8	3.4 ± 1.8
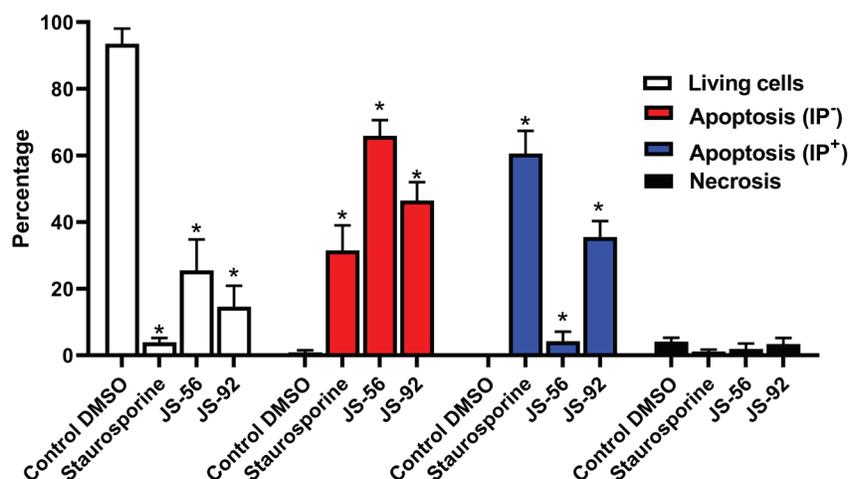
Fig. 8. Effect of tetrahydroquinolines JS-56 and JS-92 on DNA fragmentation in MCF-7 cells. The MCF-7 cells were incubated with Fluorescein-12-dUTP (fragmented DNA marker) and Propidium Iodide (IP, core marker). Cells were treated with staurosporine (1 μM), JS-56 (10 μM), and JS-92 (5 μM). The bars represent the mean ± SD derived from three independent experiments. * $p < 0.0001$ compared to the control of cells treated with DMSO.
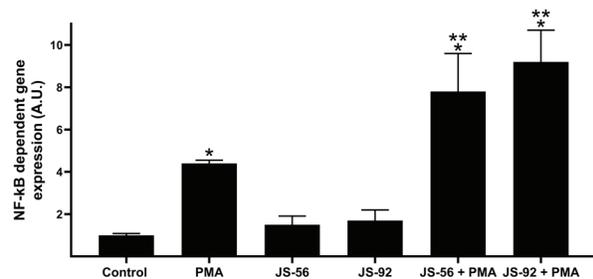
Fig. 9. Effect of tetrahydroquinolines JS-56 and JS-92 on NF-κB-dependent gene expression. HeLa tumor cells were transfected with a luciferase reporter gene under the control of the IL-6 promoter, which contains critical binding sites for NF-κB. Control, untreated MCF-7 cells; PMA, phorbol 12-myristate 13-acetate. * and ** $p < 0.05$ compared to the control of untreated cells or treated with PMA, respectively.

reported that PKC can activate IκBs kinase complexes (IKKs), which eventually leads to NF-κB activation [36]. Interestingly, the results demonstrate that the NF-κB-dependent gene expression increased significantly when cells were treated with PMA plus JS-56 or JS-92, indicating an apparent effect of both compounds on the PKC-stimulated NF-κB-dependent gene expression.

Molecular docking

The experimental results on SERCA activity obtained for the tetrahydroquinolines JS-56 and JS-92 were confirmed using molecular docking for SERCA protein (PDB code 2AGV). Interestingly, both Tg and BHQ SERCA inhibitors showed practically the same disposition as crystallized inhibitors at the respective protein binding sites, reflecting the computational package's potential for this molecular docking. In general, the tetrahydroquinolines showed a higher preference for Tg binding sites than for the BHQ active site. This effect generates a ligand-protein complex with binding energies between -12 and -13 kcal/mol at the active sites of Tg; this is in contrast to weak docking energies found at the BHQ active site for both tetrahydroquinolines. Particularly, experimental results have demonstrated that Tg exerted a more potent inhibitory activity (IC_{50} of 0.2 nM) than BHQ (IC_{50} of 20 nM) [26]. The preference of these large tetrahydroquinolines for Tg binding sites may be associated with the larger box size than BHQ active sites, which may facilitate the stabilization of the inhibitor-protein complex for these bulky and inflexible molecules. It is

essential to mention that our analysis was focused on data obtained for the Tg active site from chain-α, which exhibited the lower binding energy complex.

DISCUSSION

Tetrahydroquinolines derivatives are an essential group of natural or synthetic compounds showing a wide range of biological activities. Numerous compounds capable of inducing a Ca^{2+} signal followed by a cellular response have been reported. Ca^{2+} is one of the essential ionic constituents in the body. It has a central regulatory role in differentiation, secretion, contraction, transcription, phosphorylation, and apoptosis processes [10]. Ca^{2+} is the component required by milk to calcify newborn bones and teeth and modulates the proliferation, differentiation, and apoptosis of mammary gland epithelial cells [37]. The modulation of Ca^{2+} homeostasis and its signaling could represent a viable therapeutic approach in the treatment and/or prevention of breast cancer. Therefore, regulators of Ca^{2+} homeostasis or its signaling in mammary gland tumors are possible targets for drugs. In this investigation, we used the tetrahydroquinolines JS-56 and JS-92, modified derivatives from clove and cinnamon plants, to study the effect of these drugs on Ca^{2+} homeostasis and its possible relationship with apoptosis in breast cancer cells MCF-7.

In the interest of evaluating the cytotoxicity of tetrahydroquinolines JS-56 and JS-92 on MCF-7 breast cancer cells, the MTT assay was developed, allowing the determination of mitochondrial viability on treated cells. Both compounds are cytotoxic to MCF-7 cells in a dose-dependent manner, with an IC_{50} of 9.74 μM and 5.031 μM for JS-56 and JS-92, respectively. This difference may be related to the bromine atom that JS-92, instead of the cyanide atom present in JS-56. IC_{50} values for these compounds in MCF-7 cells are significantly lower than those reported previously in human dermis fibro-

blast, 92.87 μM and 42.48 μM for JS-56 and JS-92, respectively [17].

Through fluorimetric techniques, we were able to perform measurements of intracellular Ca^{2+} in MCF-7 cells, aiming to find possible mechanisms of action for these compounds. The results revealed that JS-56 and JS-92 promote an increase in $[Ca^{2+}]_i$. Likewise, the Tg effect on $[Ca^{2+}]_i$ is diminished when added after the impact generated by the tetrahydroquinolines, compared to when it is initially added, allowing us to conclude that these compounds promote the release of Ca^{2+} from a compartment sensitive to Tg, namely the ER. Similar experiments were done but using a solution without $CaCl_2$. Under these experimental conditions, the maximum Ca^{2+} peaks detected with JS-56, JS-92 or Tg are considerably reduced compared to those achieved in the presence of extracellular Ca^{2+}, and instead, returning to the basal level. These results show an influx of Ca^{2+} from the outside. This effect may be caused by a store-operated Ca^{2+} Entry (SOCE) or a capacitive Ca^{2+} entry induced by emptying Ca^{2+} from the ER [19,33].

The lack of an additive effect of Tg with tetrahydroquinolines on the $[Ca^{2+}]_i$ suggests a possible similar mechanism of action. The possible inhibitory potential of these compounds on SERCA activity was examined accordingly. Both tetrahydroquinolines inhibit the enzyme activity with similar maximum inhibitory effects of 56 and 51% for JS-56 and JS-92, respectively. This effect also indicates that different from Tg, these compounds could not completely inhibit the ATPase activity. However, part of the overall effect on the onset of apoptosis is the partial inhibition of SERCA activity. As it has been shown that Tg can induce ER stress via SERCA inhibition, JS-56 and JS-92 are likely potential candidates for generating ER stress through this identical mechanism. In this context, it is worth mentioning that SERCA targeting could represent an effective therapeutic strategy in treating pathogens and cancer cells [38].

The effect of both compounds on the mitochondrial membrane $\Delta\psi_m$ was determined since the accumulation of mitochondrial Ca^{2+} is a necessary event in the initiation of apoptosis via the intrinsic pathway. The primary source of the cation derives from its transfer from the ER [39]. The results revealed that both tetrahydroquinolines generate an increase in rhodamine 123 fluorescence. Although the increment in rhodamine fluorescence caused by Tg was higher than the compounds, its effect after the addition of the tetrahydroquinolines was less pronounced, suggesting that they share part of the mechanism of action on mitochondria. The fluorescence increase after treating the cells with both Tg and tetrahydroquinolines was expected due to the partial dissipation of mitochondrial $\Delta\psi_m$. This change is generated by the entry of Ca^{2+} released from the ER [6]. When both tetrahydroquinolines were added after Tg, an additional increase in fluorescence was triggered, indicating a superior dissipation of the $\Delta\psi$. These unexpected results suggested that JS-56 and JS-92 induced a cell response independent of $[Ca^{2+}]_i$. The effects are also independent of the Ca^{2+} electrophoretic uniporter. These effects have been reported previously with concentrations higher than 1 μM [40]. Accordingly, both tetrahydroquinolines, similar to the SERCA inhibitor, could interact with the mitochondria, generating a widespread effect.

Given that the $\Delta\psi_m$ loss of the mitochondrial membrane is a hallmark event of apoptosis, the presumed activation of characteristic processes associated with programmed cell death after applying the tetrahydroquinolines was investigated. In this study, it was demonstrated that tetrahydroquinolines JS-56 and JS-92 are capable of activating caspases 7 and 9 and promoting DNA fragmentation. Activation of caspases and the percentage of cells with DNA fragmentation was higher for JS-92, which coincides with its superior cytotoxic effect. DNA fragmentation in conjunction with caspase activation and the results demonstrating that these tetrahydroquinolines cause the dissipation of mitochondria $\Delta\psi_m$ to support the conclusion that these compounds activate apoptosis in MCF-7 cells. Additionally, after the inhibition of SERCA and the consequent reduction of the $[Ca^{2+}]$ at the ER, misfolded proteins could accumulate. The unfolded protein response could be triggered, leading the cells to death [12,13]. By suppressing this enzyme's activity and promoting the cation's entry into the mitochondria, the release of pro-apoptotic factors from this organelle would be facilitated [15]. Thus, part of the potential anticancer effect of these compounds would be mediated through SERCA inhibition. Based on the accumulated evidence, we suggest that disturbances of the Ca^{2+} signal induced by these tetrahydroquinolines would trigger apoptosis by promoting ER stress and the release of proapoptotic factors from the mitochondria after the entry of Ca^{2+} into this organelle.

According to our results, JS-56 and JS-92 failed to elevate the NF-κB-dependent gene expression. However, NF-κB-dependent gene expression was augmented when cells were treated with PMA, an activator of PKC which upregulates NF-κB [35]. Interestingly, the NF-κB-dependent gene expression is further elevated when cells were exposed to the combination of PMA and tetrahydroquinolines, possibly because these compounds enhance the affinity of PKC for PMA or modulate the PMA activity making it more potent and/or stable. Since NF-κB is a regulator of the expression of multiple genes, additional experiments are needed to determine its putative participation in pro-apoptotic events. We do not rule out non-specific binding of other transcription factors to this NF-κB binding site on the IL-6 promoter. Future research will confirm the participation of this transcription factor by determination of cytoplasmic/nuclear levels of p65 as well as confirmation of these results in breast cancer cells.

Based on the results that both tetrahydroquinolines may interact with the Tg bind-

ing site of SERCA, we used a docking model to test the possibility of interaction. It should be noted that both tetrahydroquinolines exhibited docking energies higher than Tg, indicating that the Tg-Ca^{2+}-ATPase complex is more stable than the quinoline-Ca^{2+}-ATPase complex (Table 1). These theoretical findings are in good agreement with experimental data, where Tg exhibited the higher experimental inhibitory activity (IC$_{50}$ of 0.2 nM) compared to the tested tetrahydroquinolines (IC$_{50}$ of 60 and 100 μM for JS-56 and JS-92, respectively). The high stabilization of the Tg-Ca^{2+}-ATPase complex can be asso-

ciated with diverse intermolecular interactions with residues located in the Tg1 active site, including (i) a large number of hydrophobic interactions with at least 20 residues in chain A and 13 residues in chain B; (ii) from one to two strong *H*-interactions with Ile-829 and Phe-834 for JS-56 and JS-92, respectively; and (iii) *H-π* interactions between phenolic, quinolinic, or indolic rings with specific phenyl rings in Phe-834, Phe-256 or Tyr-837 (Table 1 and Fig. 10). However, it is essential to mention that these diverse interactions found for these tetrahydroquinolines are located in turn to a specific re-
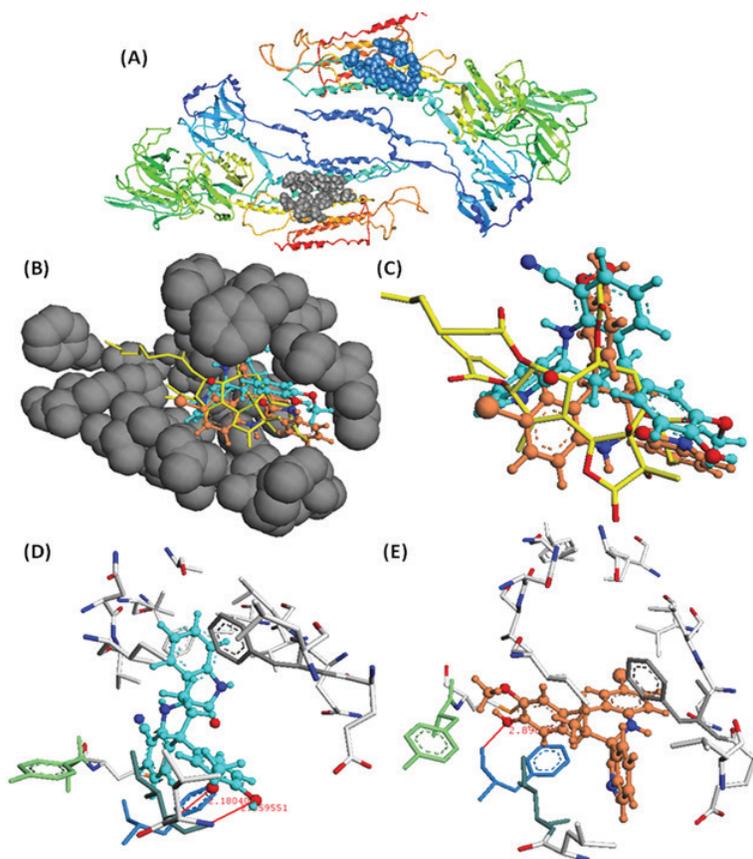
Fig. 10. Molecular docking of the tetrahydroquinolines JS-56 and JS-92 on the TG1 active site. (A) TG1 (gray ribbons) and TG2 (blue ribbons) active sites into SERCA protein; (B) Location of JS-56 (cyan color) and JS-92 (orange color) into the TG1 active site pocket of SERCA protein; (C) Superimposition between JS-56 (cyan) and JS-92 (orange) with TG1 substrate (yellow color); (D) Disposition and interactions of JS-56 (cyan) (D) and JS-92 (orange) (E) into TG1 active site. Tentative H-π interactions between phenolic, indolic, or quinolinic rings of JS-56 and JS-92 with Phe-236 (gray color), Phe-834 (blue color), and Phe-256 (green color) residues.

gion of the active site. At the same time, Tg, bearing a highly flexible octanoic acid residue at C2, makes hydrophobic contacts with non-polar patches on the outer surface of SERCA's trans-membrane domain and possibly with surrounding lipids, facilitating the stabilization of the ligand-protein complex. The molecular docking analysis shows that hydrophobic ligands containing long and flexible side chains are needed to design effective inhibitors of the Ca^{2+}-ATPase enzyme due to the high hydrophobic and extended nature of the Ca^{2+}-ATPase active site. Future studies will continue to evaluate these types of compounds and their effect on Ca^{2+} and apoptosis, developing new analogs with different types of chemical modifications on a more diverse panel of breast cancer cells and other types of malignancies.

Both tetrahydroquinolines derivatives, JS-56 and JS-92, induced cell death in MCF-7 cells through a combination of events. These events include the elevation of the $[Ca^{2+}]_i$, inhibiting SERCA via direct interaction, partially damaging the mitochondria, which induced activation of apoptotic pathways and consequently MCF-7 cell death. Therefore, these results show the potential that these types of compounds would have in anti-neoplastic treatment in humans. It is hoped that more powerful analogs can be developed in the future.

Funding

Conflict of interest

The authors declare no conflicts of interest.

Authors contributions

SM: Investigation, Methodology, Data curation, Writing – original draft, Writing – review & editing. AM: Methodology, Writing – review & editing. LC: Methodology, Writing – review & editing. FS: *In silico* analysis, Writing – review & editing. AP: NF-κB gene expression analysis. VK: *In silico* analysis, isolation and purification of natural compounds. DMA: Isolation and purification of natural compounds. AR: Methodology, Writing – review & editing. FA: *In silico* analysis, Writing – review & editing. JS: Flow cytometry analysis, Writing – review & editing. GB: Conceptualization, Formal analysis, Supervision, Funding acquisition, Writing – review & editing.

Author's ORCID numbers

- Semer Maksoud:
  0000-0001-9773-9415

- Adriana Mayora:
  0000-0002-6817-2066

- Laura Colman:
  0000-0002-5188-880X

- Felipe Sojo:
  0000-0002-6559-4845

- Adriana A. Pimentel:
  0000-0002-8862-9318

- Vladimir V. Kouznetsov:
  0000-0003-1417-8355

- Diego R. Merchán-Arenas:
  0000-0001-9243-5914

- Ángel H. Romero:
  0000-0001-8747-5153V

- Francisco Arvelo:
  0000-0003-1590-358x

- Juan Bautista De Sanctis:
  0000-0002-5480-4608

- Gustavo Benaim:
  0000-0002-9359-5546

REFERENCES

1. **World Health Organization (WHO).** Breast Cancer (December 2021). https://www.who.int/news-room/fact-sheets/detail/breast-cancer.

2. **Peart O.** Breast intervention and breast cancer treatment options. Radiol Technol 2015;86:535M-558M; quiz 559–62.

3. **Sergeev IN, Li S, Colby J, Ho C-T, Dushenkov S.** Polymethoxylated flavones induce Ca^{2+}-mediated apoptosis in breast cancer cells. Life Sci 2006;80:245–253.

4. **Sareen D, Darjatmoko SR, Albert DM, Polans AS**. Mitochondria, calcium, and calpain are key mediators of Resveratrol-induced apoptosis in breast cancer. Mol Pharmacol 2007;72:1466–1475.

5. **Lee J-H, Li Y-C, Ip S-W, Hsu S-C, Chang N-W, Tang N-Y, Yu C-S, Chou S-T, Lin S-S, Lino C-C, Yang J-S, Chung J-G.** The role of Ca^{2+} in baicalein-induced apoptosis in human breast MDA-MB-231 cancer cells through mitochondria- and caspase-3-dependent pathway. Anticancer Res 2008;28:1701–1711.

6. **Pimentel AA, Felibertt P, Sojo F, Colman L, Mayora A, Silva ML, Rojas H, Dipolo R, Suarez AI, Compagnone RS, Arvelo F, Galindo-Castro I, De Sanctis JB, Chirino P, Benaim G.** The marine sponge toxin agelasine B increases the intracellular Ca^{2+} concentration and induces apoptosis in human breast cancer cells (MCF-7). Cancer Chemother Pharmacol 2012;69:71–83.

7. **Zhang Z, Teruya K, Eto H, Shirahata S.** Induction of apoptosis by low-molecular-weight fucoidan through calcium- and caspase-dependent mitochondrial pathways in MDA-MB-231 breast cancer cells. Biosci Biotechnol Biochem 2013;77:235–242.

8. **Al-Taweel N, Varghese E, Florea A-M, Büsselberg D.** Cisplatin (CDDP) triggers cell death of MCF-7 cells following disruption of intracellular calcium ($[Ca^{2+}]i$) homeostasis. J Toxicol Sci 2014;39:765–774.

9. **Sehgal P, Szalai P, Olesen C, Praetorius HA, Nissen P, Christensen SB, Engedal N, Møller J V.** Inhibition of the sarco/endoplasmic reticulum (ER) Ca^{2+}-ATPase by thapsigargin analogs induces cell death via ER Ca^{2+} depletion and the unfolded protein response. J Biol Chem 2017;292:19656–19673.

10. **Carafoli E.** Calcium signaling: A tale for all seasons. Proc Natl Acad Sci 2002;99:1115–1122.

11. **Carafoli E**. Intracellular calcium homeostasis. Annu Rev Biochem 1987;56:395–433.

12. **Breckenridge DG, Germain M, Mathai JP, Nguyen M, Shore GC**. Regulation of apoptosis by endoplasmic reticulum pathways. Oncogene 2003;22:8608–8618.

13. **Szegezdi E, Logue SE, Gorman AM, Samali A.** Mediators of endoplasmic reticulum stress-induced apoptosis. EMBO Rep 2006;7:880–885.

14. **Rizzuto R, Bernardi P, Pozzan T.** Mitochondria as all-round players of the calcium game. J Physiol 2000;529:37–47.

15. **Hengartner MO.** The biochemistry of apoptosis. Nature 2000;407:770–776.

16. **Kouznetsov V V, Bello Forero JS, Amado Torres DF.** A simple entry to novel spiro dihydroquinoline-oxindoles using Povarov reaction between 3-N-aryliminoisatins and isoeugenol. Tetrahedron Lett 2008; *doi: 10.1016/j.tetlet.2008.07.096.*

17. **Kouznetsov V, R. Merchan Arenas D, Arvelo F, S. Bello Forero J, Sojo F, Munoz A**. 4-Hydroxy-3-methoxyphenyl substituted 3-methyl-tetrahydroquinoline derivatives obtained through Imino Diels-Alder reactions as potential antitumoral agents. Lett Drug Des Discov 2010;7:632–639.

18. **Mosmann T.** Rapid colorimetric assay for cellular growth and survival: Application to proliferation and cytotoxicity assays. J Immunol Methods 1983;65:55–63.

19. **Colina C, Flores A, Castillo C, Rosario Garrido M del, Israel A, DiPolo R, Benaim G.** Ceramide-1-P induces Ca^{2+} mobilization in Jurkat T-cells by elevation of Ins(1,4,5)-P3 and activation of a store-operated calcium channel. Biochem Biophys Res Commun 2005;336:54–60.

20. **Grynkiewicz G, Poenie M, Tsien RY**. A new generation of Ca^{2+} indicators with greatly improved fluorescence properties. J Biol Chem 1985;260:3440–3450.

21. **Eletr S, Inesi G.** Phospholipid orientation in sacroplasmic membranes: Spin-label ESR and proton NMR studies. Biochim Biophys Acta - Biomembr 1972;282:174–179.

22. **Fiske CH, Subbarow Y**. The colorimetric determination of phosphorus. J Biol Chem 1925;66:375–400.

23. **Benaim G, Cervino V, Lopez-Estraño C, Weitzman C**. Ethanol stimulates the plasma membrane calcium pump from human erythrocytes. Biochim Biophys Acta - Biomembr 1994;1195:141–148.

24. **Benaim G, Sanders JM, Garcia-Marchán Y, Colina C, Lira R, Caldera AR, Payares G, Sanoja C, Burgos JM, Leon-Rossell A, Concepcion JL, Schijman AG, Levin M, Oldfield E, Urbina JA.** Amiodarone has intrinsic anti-Trypanosoma cruzi activity and acts synergistically with posaconazole. J Med Chem 2006;49:892–899.

25. **Kagawa S, Gu J, Honda T, McDonnell TJ, Swisher SG, Roth JA, Fang B**. Deficiency of caspase-3 in MCF7 cells blocks Bax-mediated nuclear fragmentation but not cell death. Clin Cancer Res 2001;7:1474–1480.

26. **Obara K, Miyashita N, Xu C, Toyoshima I, Sugita Y, Inesi G, Toyoshima C.** Structural role of countertransport revealed in Ca^{2+} pump crystal structure in the absence of Ca^{2+}. Proc Natl Acad Sci 2005;102:14489–14496.

27. **Guex N, Peitsch MC.** SWISS-MODEL and the Swiss-Pdb Viewer: An environment for comparative protein modeling. Electrophoresis 1997;18:2714–2723.

28. **Fusi F, Saponara S, Gagov H, Sgaragli G.** 2,5-Di-t-butyl-1,4-benzohydroquinone (BHQ) inhibits vascular L-type Ca^{2+} channel via superoxide anion generation. Br J Pharmacol 2001;133:988–996.

29. **Lytton J, Westlin M, Hanley MR**. Thapsigargin inhibits the sarcoplasmic or endoplasmic reticulum Ca-ATPase family of calcium pumps. J Biol Chem 1991;266:17067–17071.

30. **Thompson M**. ArgusLab 4.0 Planaria Software. LLC: Seatle, WA. 2004.

31. **Becke AD**. A new mixing of Hartree–Fock and local density-functional theories. J Chem Phys 1993;98:1372–1377.

32. **Young DC**. Computational Drug Design. Hoboken, NJ, USA: John Wiley & Sons, Inc., 2009.

33. **Colina C, Flores A, Rojas H, Acosta A, Castillo C, Rosario Garrido M del, Israel A, DiPolo R, Benaim G.** Ceramide increase cytoplasmic Ca^{2+} concentration in Jurkat T cells by liberation of calcium from intracellular stores and activation of a store-operated calcium channel. Arch Biochem Biophys 2005;436:333–345.

34. **Moore GA, McConkey DJ, Kass GEN, O'Brien PJ, Orrenius S.** 2,5-Di(tert-butyl)-1,4-benzohydroquinone - a novel inhibitor of liver microsomal Ca^{2+} sequestration. FEBS Lett 1987;224:331–336.

35. **Tang D, Lahti JM, Kidd VJ.** Caspase-8 activation and bid cleavage contribute to MCF7 cellular execution in a caspase-3-dependent manner during staurosporine-mediated apoptosis. J Biol Chem 2000;275:9303–9307.

36. **Schmitz ML, Bacher S, Dienz O.** NF-κB activation pathways induced by T cell costimulation. FASEB J 2003;17:2187–2193.

37. **Lee WJ, Monteith GR, Roberts-Thomson SJ.** Calcium transport and signaling in the mammary gland: Targets for breast cancer. Biochim Biophys Acta - Rev Cancer 2006;1765:235–255.

38. **Tadini-Buoninsegni F, Smeazzetto S, Gualdani R, Moncelli MR**. Drug interactions with the Ca^{2+}-ATPase from sarco(endo)plasmic reticulum (SERCA). Front Mol Biosci 2018;5:36.

39. **Demaurex N.** Cell biology: Apoptosis--the calcium connection. Science 2003;300:65–67.

40. **Vercesi AE, Moreno SN, Bernardes CF, Meinicke AR, Fernandes EC, Docampo R.** Thapsigargin causes Ca^{2+} release and collapse of the membrane potential of Trypanosoma brucei mitochondria in situ and of isolated rat liver mitochondria. J Biol Chem 1993;268:8564–8568.